Statistical properties of the spectrum of the extended Bose–Hubbard model



J. Stat. Mech. (2010) P08011

(http://iopscience.iop.org/1742-5468/2010/08/P08011)

Journal of Statistical Mechanics: Theory and Experiment
An IOP and SISSA journal

# Statistical properties of the spectrum of the extended Bose–Hubbard model

**Corinna Kollath[1], Guillaume Roux[2,3], Giulio Biroli[4] and Andreas M Läuchli[5]**

[1] Centre de Physique Théorique, CNRS, École Polytechnique, F-91128 Palaiseau Cedex, France
[2] Laboratoire de Physique Théorique et Modèles Statistiques, Université Paris-Sud, UMR8626, F-91405 Orsay, France
[3] CNRS, F-91405 Orsay, France
[4] Institut de Physique Théorique, CEA/DSM/IPhT-CNRS/URA 2306 CEA-Saclay, F-91191 Gif-sur-Yvette, France
[5] Max-Planck-Institut für Physik komplexer Systeme, D-01187 Dresden, Germany
E-mail: Corinna.Kollath@cpht.polytechnique.fr, guillaume.roux@u-psud.fr, giulio.biroli@cea.fr and laeuchli@comp-phys.org

Received 13 April 2010
Accepted 14 July 2010
Published 12 August 2010

Online at stacks.iop.org/JSTAT/2010/P08011
doi:10.1088/1742-5468/2010/08/P08011

**Abstract.** Motivated by the role that spectral properties play for the dynamical evolution of a quantum many-body system, we investigate the level spacing statistics of the extended Bose–Hubbard model. In particular, we focus on the distribution of the ratio of adjacent level spacings, useful at large interactions, to distinguish between chaotic and non-chaotic regimes. After revisiting the bare Bose–Hubbard model, we study the effect of two different perturbations: next-nearest-neighbor hopping and nearest-neighbor interaction. The system size dependence is investigated together with the effect of the proximity to integrable points or lines. Lastly, we discuss the consequences of a cutoff in the number of onsite bosons on the level statistics.

**Keywords:** Hubbard model (theory), quantum chaos, connections between chaos and statistical physics, optical lattices


1742-5468/10/P08011+18$30.00

## Contents



## 1. Introduction

In classical systems, the chaotic nature of a Hamiltonian plays a crucial role in determining the dynamics. Chaotic systems explore a large area of their phase space, whereas non-chaotic ones can be trapped in certain atypical subspaces [1]. Thus, chaos plays a considerable role in explaining thermalization and ergodicity. For quantum systems the situation is less clear. In principle, the quantum dynamics is linear, since it follows the Schrödinger equation, and therefore the notion of chaos is not so well defined. However, in quantum systems for which a classical counterpart exists, one finds that the dynamics is very different, depending on whether the corresponding classical motion is chaotic or regular [1]. For generic quantum systems, chaos is also believed to be essential for thermalization [2, 3] and delocalization in Fock space [4]. The recent realization of closed quantum systems out of equilibrium by strongly correlated cold atom clouds [5] have led to a renewal of interest in the chaotic properties of many-body quantum systems and their relation to thermalization [6].

For chaotic quantum systems it has been conjectured that their spectra show universal features which are related to the theory of random matrices [7]–[10]. To quantify the spectral properties of a given Hamiltonian, a natural quantity to look at is the gap between adjacent many-body levels $\delta_n = E_{n+1} - E_n$, where $\{E_n\}$ is the list of eigenvalues in ascending order. The general symmetries of the Hamiltonian, like time-reversal and half-integer-spin rotational invariance, determine the random matrix ensemble (among orthogonal, unitary and symplectic ensembles) to which it belongs [7]. A spinless time-reversal invariant Hamiltonian such as the Bose–Hubbard model (for generic parameters) should have similar universal features as the Gaussian orthogonal ensemble (GOE). For example, the adjacent level spacing distribution $P_\Delta(\delta)$ is predicted to take the Wigner–Dyson form:

$$P_\Delta(\delta) = \frac{\pi}{2}\frac{\delta}{\Delta}\exp\left(-\frac{\pi}{4}\frac{\delta^2}{\Delta^2}\right), \tag{1}$$



J. Stat. Mech. (2010) P08011

where $\Delta$ is the mean level spacing. In contrast for so-called integrable models, in which the properties of the system are determined by an extensive number of conserved quantities, the level spacings should exhibit the following Poissonian distribution:

$$P_\Delta(\delta) = \exp\left(-\delta/\Delta\right). \tag{2}$$

The relation between the spectral properties of a quantum system and the random matrix ensembles has been demonstrated numerically even for strongly correlated many-body systems without classical counterparts. In particular a GOE-like behavior was pointed out for the non-integrable two-dimensional $t$–$J$ model [11]. In one-dimensional models, it was checked that at, and close to, the integrable points, the statistics was Poissonian-like [12]. In one dimension, non-diffractive models are integrable on rigorous grounds and solvable using the Bethe ansatz which provides all eigenstates [13]. Several other systems have been discussed since then [1, 10, 14, 15]. Therefore, analyzing the spectral properties of a system provides a phenomenological approach to investigate the chaotic nature of the quantum Hamiltonian.

In this work we consider the properties of the spectrum of the Bose–Hubbard model. This model is a paradigmatic strongly correlated many-body system where interactions of amplitude $U$ compete with the kinetic energy favored by the hopping $J$. It appeared in several contexts of condensed matter theory and regained a lot of interest since it has been realized in quantum gases confined to artificial lattice structures [5]. Its out-of-equilibrium dynamics, and in particular the question of thermalization following a quantum quench, have also been studied numerically [16]–[20]. As perturbations to the Bose–Hubbard Hamiltonian are experimentally relevant in different regimes [21], it is essential to address the sensitivity of the spectral features to extra terms. We consider the effect of two different perturbations and their consequences on the level statistics. We focus on the model with a next-nearest-neighbor hopping with amplitude $J_2$ as well as a nearest-neighbor interaction with amplitude $V$. The Hamiltonian under study then is

$$H = -J\sum_{j=1}^{L}\left(b_j^\dagger b_{j+1} + \text{h.c.}\right) - J_2\sum_{j=1}^{L}\left(b_j^\dagger b_{j+2} + \text{h.c.}\right) + \frac{U}{2}\sum_{j=1}^{L}\hat{n}_j(\hat{n}_j - 1) + V\sum_{j=1}^{L}\hat{n}_j\hat{n}_{j+1}, \tag{3}$$

where $b_j^\dagger$ and $b_j$ are the bosonic creation and annihilation operators, $\hat{n}_j = b_j^\dagger b_j$ are the number operators on site $j$ and $L$ is the number of sites in the chain. Periodic boundary conditions are used to take advantage of translational invariance. We analyze the spectrum in the subspace spanned by reflection symmetric states with zero total momentum using full exact diagonalization. No cutoff in the onsite occupation $M$ is assumed, i.e. $M = N$, and unit filling $N/L = 1$ is taken if not stated otherwise ($N$ is the total number of bosons). The symmetrized Hilbert space has dimensions up to 56 822 for $N = L = 12$. The considered extended Bose–Hubbard model is integrable (in a broad sense) only in the two limiting cases of $U = V = 0$ (free bosons) and $J = J_2 = 0$ (atomic limit).

In a first analysis on small lattices, Kolovsky and Buchleitner [22] discussed the chaotic behavior of the bare Bose–Hubbard model ($V = J_2 = 0$). They investigated the level statistics and the Shannon entropy of the eigenstates with respect to the basis of the two integrable limits as a probe of the eigenstate delocalization (another chaotic feature). A pronounced similarity of the level statistics with GOE and a maximal Shannon entropy



J. Stat. Mech. (2010) P08011

has been found when the hopping amplitude and the interaction strength are of the same order. Furthermore, it has been noticed that the low and very high energy parts of the spectrum seem to display features of integrable spectra. A chaotic trimeric version of the Bose–Hubbard model has also been analyzed [23, 24] and a comparison to the semiclassical approximation has been carried out when $N/L \gg 1$. Another case that has been studied corresponds to restricting the maximum onsite number of bosons $M$ to one. In this case, the Bose–Hubbard model boils down to a hard-core boson model (XXZ) which has the particularity of being integrable provided $J_2 = 0$. The level statistics of this hard-core model, perturbed by a non-integrable operator, has been studied recently [25]. While the two models are physically equivalent in the low energy physics provided that $U$ is large enough, the high energy spectra are very different even in the large-$U$ limit.

In this paper, we analyze the level statistics of the extended Bose–Hubbard model in detail, using system sizes up to $L = N = 12$ sites. All data are restricted to the zero-momentum and reflection symmetric sector (that of the ground state). In section 2 we study both the level spacing distribution and the distribution of the ratio of consecutive level spacings. The latter is a very useful observable, in particular close to the atomic limit. This allows us to address the energy and finite size dependences. Furthermore, we investigate in section 3 the influence of different perturbations on the spectrum of the Bose–Hubbard model. We consider a next-nearest-neighbor hopping and a nearest-neighbor interaction and the focus is put on how the chaotic features evolve away from integrable points (lines) in the parameter space. Lastly, we discuss the effect of the onsite occupation cutoff $M$ on the level statistics.

## 2. Properties of the bare Bose–Hubbard model

We first focus on the bare Bose–Hubbard model ($J_2 = V = 0$) [22]. In figure 1, typical level spacing distributions of the unfolded spectrum are shown for two different interaction strengths. In order to remove the dependence on the system specific mean level density, the 'unfolding' procedure consists in renormalizing the level spacings by using a suitable fit for the smooth part (see [10] for details of the procedure). The left panel of figure 1 shows that the distribution for $U/J = 2$ closely follows the Wigner–Dyson distribution of the GOE. In particular, the distribution vanishes for small level spacings, a typical signature of level repulsion associated with avoided level crossings. When approaching the integrable points the distribution deviates from Wigner–Dyson. This is shown for strong interaction $U/J = 40$ in the right panel of figure 1, but occurs also when lowering the interaction. The tail of the distribution is close to the exponential tail of the Poisson distribution; for small level spacings there is a significant enhancement compared to the GOE distribution but some level repulsion persists. We observe that increasing the size of the system (not shown, see also the discussion hereafter) tends to increase the similarity to the Wigner–Dyson distribution. In particular, the repulsion at small level spacings becomes more and more pronounced. However, for currently accessible system sizes, it is not clear whether the distribution very close to the integrable points will converge to the Wigner–Dyson one.

The study of systems with large interaction strength is involved due to the appearance of a band structure in the density of states (see figure 2). The spectrum evolves from a smooth broad spectrum for small interaction strength to a series of narrow energy bands



J. Stat. Mech. (2010) P08011

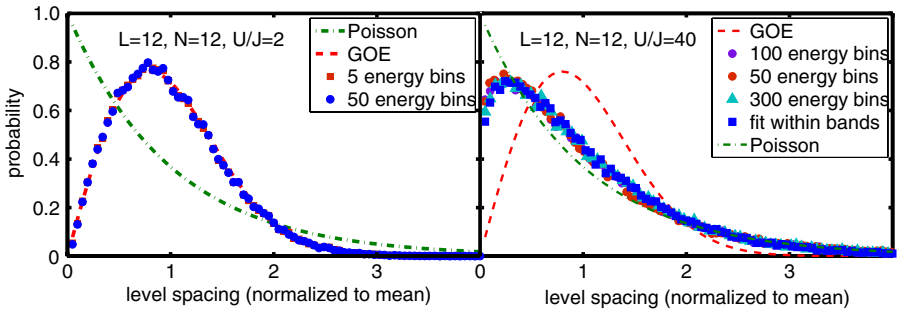


**Figure 1.** The level spacing distribution for $U/J = 2$ and $U/J = 40$ for a system of length $L = 12$ is shown (symbols). The dashed–dotted green curve is the Poisson distribution and the dashed red curve the Wigner–Dyson distribution of a purely GOE-like ensemble. The different symbols correspond to different unfolding procedures. For the curves labeled by the number of energy bins, the unfolding is performed locally over energy regions, which divides the total energy range covered by the eigenvalues into equally spaced energy bins. The smooth part of the level staircase is fitted by a polynomial. Additionally an unfolding within the energy bands is performed for $U/J = 40$ using the function $A2 + (A1 - A2)/(1 + \exp((E - E_0)/\mathrm{d}E))$, where $A1$, $A2$, $E_0$ and $\mathrm{d}E$ are fitting parameters.

separated by $U$ for large interaction strength[6]. This would make the unfolding complicated because it is difficult to separate the spectrum into a smooth and a fluctuating part. To obtain reliable results we performed different unfolding procedures fitting locally different parts of the spectrum. If the ranges over which the fits are performed are chosen in a suitable way, the same general form of the spectra is recovered, even though small discrepancies can occur. Note that the complicated form of the density of states also makes a study of longer range correlations of the spectrum involved.

To avoid this complication, we continue our study using another measure which has the advantage of not depending on the unfolding procedure: the ratio of consecutive gaps between adjacent levels [26]. This quantity is defined by $r_n = \min(\delta_n, \delta_{n-1})/\max(\delta_n, \delta_{n-1})$. As long as the density of states does not vary on the scale of the mean level spacing, the trivial dependence on the smooth part drops out and there is no need for unfolding. This is exemplified in figure 3, where we compare for a GOE random matrix ensemble the distribution of the level spacing and of the ratio of the consecutive level spacings taken over two different energy ranges without performing the unfolding procedure. The first energy range lies at the boundary of the spectrum where the density of states varies considerably. In contrast, the second energy range is situated in the center of the spectrum, where the density of states exhibits only slow changes. The GOE distribution is computed numerically as in [26] using the averaged results of 10 000 samples of random matrices of size $5000^2$. It is clearly seen that the ratio of consecutive level spacings does not depend on the region used, whereas the level spacing statistics is different for the two chosen regions due to its strong dependence on the smooth part of the spectrum. The local ratio

[6] However, note that the mean level spacing is still much smaller than the width of the energy bands.



J. Stat. Mech. (2010) P08011

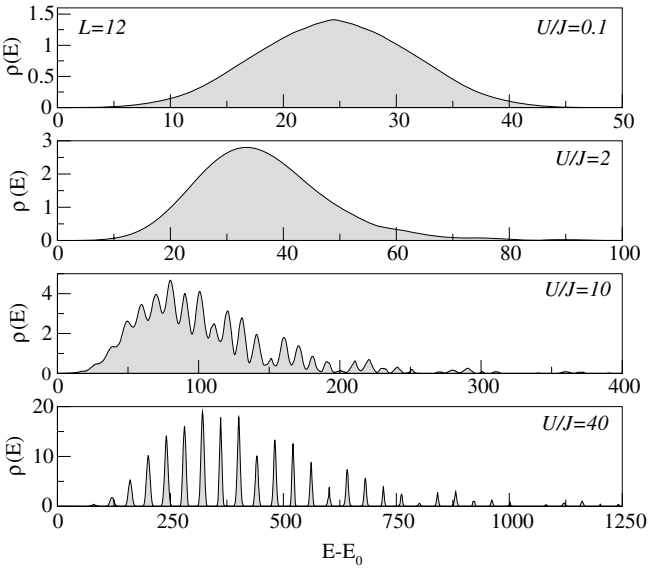


**Figure 2.** The many-body density of states $\rho$ in the zero-momentum and reflection symmetric sector and for different interaction strengths. $E_0$ is the ground state energy. The evolution from a smooth spectrum at low interaction strength to the appearance of well-separated energy bands at large interaction strength is shown. The smooth curves are obtained broadening the $\delta$ peaks by Gaussians ($\bar{\rho}(E) = \sum_n g_\Delta(E - E_n)$ with $g_\Delta$ a Gaussian of width $\Delta$). However, note that even for large interaction strengths the width of the Gaussians is much smaller than the width of the energy bands.

of consecutive level spacings averaged over the GOE ensemble is also independent of the density of states (left panel of figure 3). On the basis of these results, which show that $r$ is a useful random variable to analyze the spectral statistics, we continue our study focusing on the ratio of consecutive gaps.

We give in the left panel of figure 4 typical distributions $P(r)$ obtained for the Bose–Hubbard model at different interaction strength. As expected, the $P(r)$ distribution depends on the chaoticity of the Hamiltonian: the distribution for a Poissonian spectrum is $P(r) = 2/(1 + r)^2$ while it can been computed numerically for the GOE ensemble (figures 3 and 4). As for the level spacing distribution, the maximum resemblance with GOE is observed when $U \simeq J$. In the proximity of the two integrable limits $U = 0$ and $J = 0$ the distributions approach the Poisson prediction, particularly on the tail. We checked for a wide range of values of $U$ that the distribution of these ratios is in good agreement with the level spacing distribution using different local unfolding procedures.

In order to have a systematic tool to probe the proximity either to Poisson or GOE, we use the results on the mean value $\langle r \rangle$ which is $\langle r \rangle_{\mathrm{P}} = 2\ln 2 - 1 \approx 0.386$ for Poisson and $\langle r \rangle_{\mathrm{GOE}} \approx 0.53(1)$ for GOE. We thus expect that this averaged ratio should display a maximum for an interaction strength around $U \approx J$. In figure 5 this ratio is given for different interaction strengths and system lengths. At intermediate interaction strength ($0.3 < U/J < 4$) we see that $\langle r \rangle$ gets very close to the GOE prediction. Even though there



J. Stat. Mech. (2010) P08011

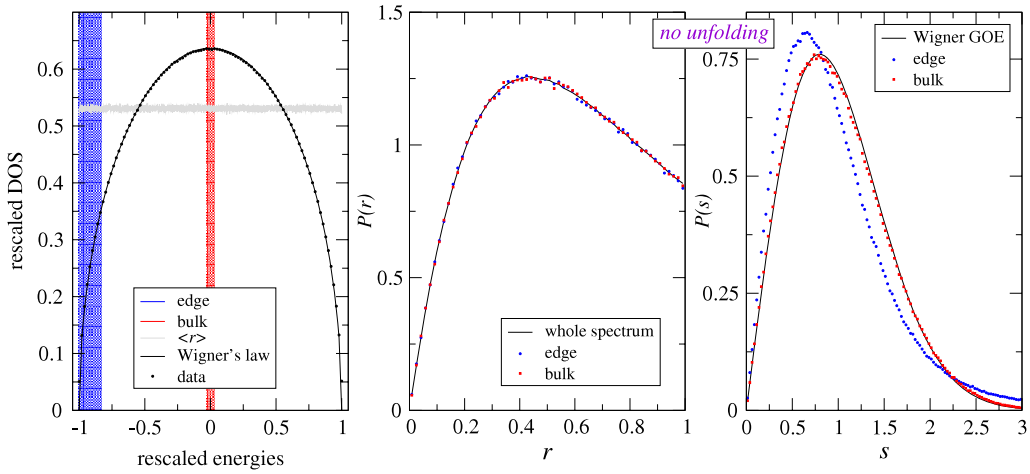


**Figure 3.** Left panel: semicircular density of state for a GOE ensemble of random matrices of size $5000^2$ averaged over 10 000 realizations. In addition, the value of the ratio of consecutive level spacings, averaged over the different realizations, is given as a function of energy, showing that it does not depend on the density of states. The shaded regions are the regions over which the distributions shown in the central and right panel are taken (they both contain 200 states). Central panel: distribution of the ratio of consecutive level spacings taken over a region at the edge, in the bulk and of the whole spectrum: the distribution does not depend on the variation of the local density of states. Right panel: distribution of the level spacing in the same regions without unfolding the spectrum showing the strong dependence on $\rho(E)$.

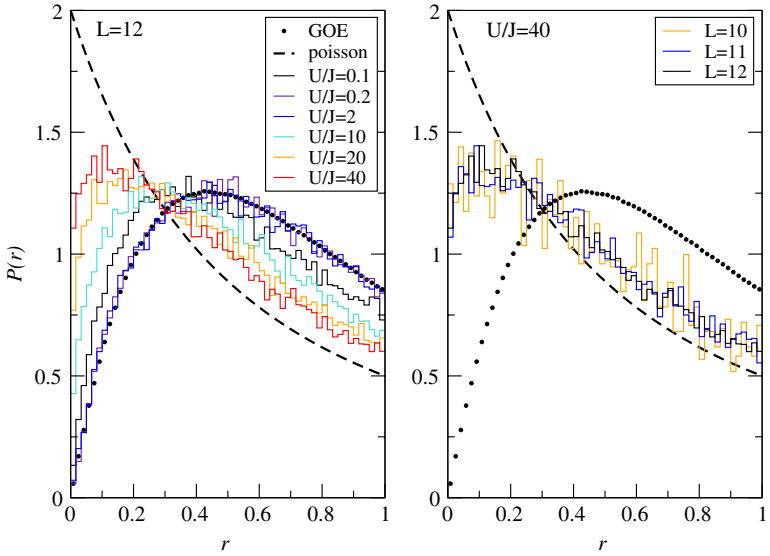


**Figure 4.** Typical distribution of the ratio of adjacent level spacings $r$. Left panel: different interaction strengths for $L = 12$ are compared with Poisson and GOE distributions. The proximity to the chaotic regime is seen when $U \simeq J$, while for $U \gg J$ and $U \ll J$ the curves approach the Poissonian tail. Right panel: system size dependence for $U/J = 40$.



J. Stat. Mech. (2010) P08011

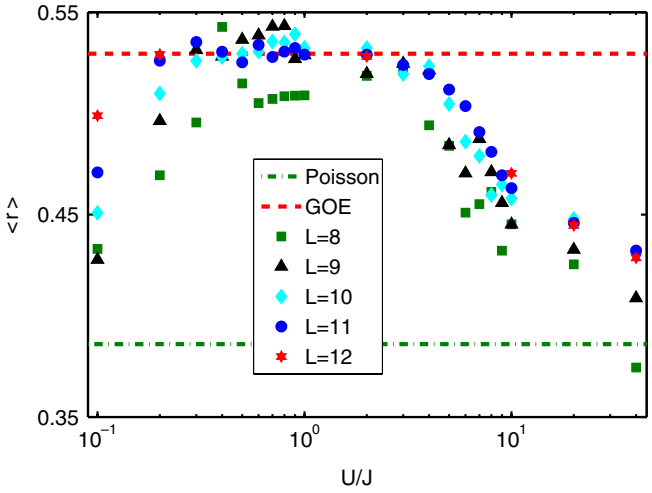


**Figure 5.** Evolution of the average ratio of consecutive level spacings $\langle r \rangle$ with the interaction strength $U/J$. For the Poisson distribution the average value of $\langle r \rangle_{\mathrm{P}} = 0.386$ and for the GOE ensemble $\langle r \rangle_{\mathrm{GOE}} = 0.53$. The average is taken for the full spectrum, without cutting the low and the high energy part. A clear tendency of larger system sizes versus the GOE ensemble value is seen.

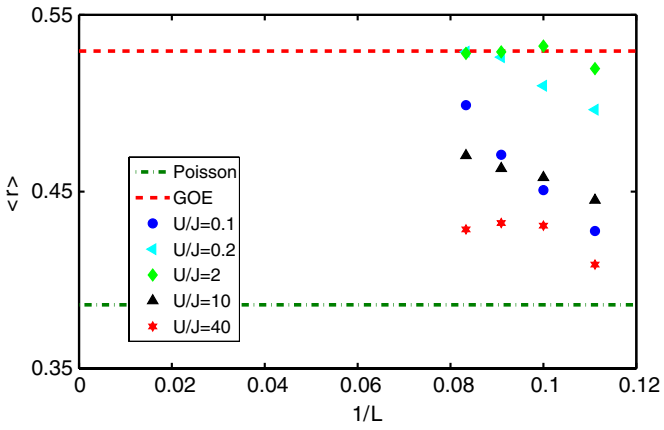


**Figure 6.** Scaling of the ratio of consecutive level spacings $\langle r \rangle$ with the inverse system size for different interaction strength.

is a small system size dependence left, the values for the longer system sizes considered are quite close to the expected value. For small and large values of the interaction strength we see that the behavior is different. For these regimes the values of $\langle r \rangle$ lie in between the ones expected for the GOE and the Poisson ensemble and for most of these values a strong system size dependence is still evident. Typically, the trend for longer system sizes goes towards $\langle r \rangle_{\mathrm{GOE}}$, as shown in figure 6 for some chosen values of the interaction. This suggests that, away from the integrable points, some critical length scale (or particle number) exists above which the system shows a level statistics which is very close to the one of the GOE ensemble. Our results further suggest that this length scale possibly grows in the proximity of the integrable points. For instance, when $U/J = 40$, the distributions



J. Stat. Mech. (2010) P08011

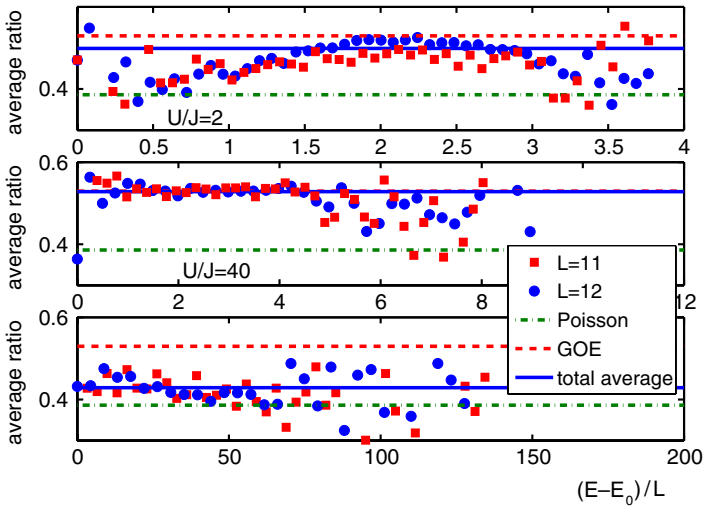


**Figure 7.** Average ratio of consecutive level spacings taken in different energy intervals of equal size for different interaction strength $U/J = 0.1, 2, 40$ and different system length $L = 11, 12$. The number of bins taken for the average is 50.

hardly evolve with the system size (see figure 4 right panel). We expect that, for large enough sizes, the properties of the spectrum might well be described by a GOE. However, the question whether or not a finite deviation of the parameters from the integrable limit is necessary to obtain GOE-like characteristics cannot be conclusively answered[7]. Still, the obtained results can be compared with other scenarios on the effect of the interaction in the Bose–Hubbard model. For instance, Cassidy *et al* suggested [27] that there could be an interaction threshold in the Bose–Hubbard model for the chaotic behavior to develop, based on calculations valid in the semiclassical limit $N/L \gg 1$ supplemented by a mean-field calculation. Extrapolating their results to the $N = L$ limit, the threshold would be $U/J \simeq 0.5$. In contrast, our results demonstrate that for low filling $n = 1$ even at $U/J \simeq 0.1$, the level statistics features have a strong tendency towards chaotic behavior and no signature of a threshold is found.

Up to now we have considered the properties of the whole spectrum. However, the question arises how these properties change within different energy ranges of the spectrum. To illustrate this, we show in figure 7 the average ratio taken over different ranges of the spectrum[8]. We must notice that, contrary to the GOE benchmark of figure 3, the Hamiltonian is deterministic and no sampling can smooth the curves: we were able to get good statistics only by reaching large enough system sizes. For small values of the interaction strength ($U/J = 0.1$ and $U/J = 2$ in figure 7) the average ratio slightly depends on the energy and one can observe that the bulk of the spectrum displays the GOE prediction while edges show some deviations with strong fluctuations. These strong

[7] Notice that the scaling analysis of the level statistics have some strong numerical limitations. Indeed, as the width of the spectrum scales as $N^2$ while the number of states scales exponentially with $N$, we may expect the minimal level spacing to reach the numerical accuracy of full diagonalization at some relatively small system size $L$. However, these system sizes are longer than the system sizes considered here.

[8] We checked that the ratio exhibits the same features as the level spacing statistics.

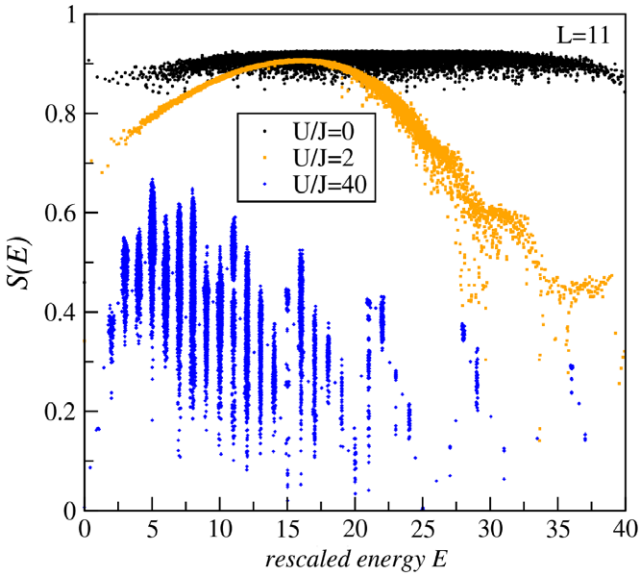


**Figure 8.** The Shannon entropy in the real-space symmetrized basis of exact diagonalization is shown for different interaction strengths. An evolution from a smooth behavior for small interaction strength towards a very fluctuating behavior for large interaction strength can be seen.

fluctuations may be attributed either to the fact that the small density of states induces bad statistics or to the fact that the physics at the edges (in particular, close to the ground state) display different statistics than for the high energy excited states in the bulk. A clear maximum exists in the central region. Increasing the system size for $U/J = 0.1$ makes the bulk value closer to the GOE prediction. For intermediate values of the interaction strength $U/J = 2$ (central panel, figure 7) the properties of the spectrum do not change much in different energy regions and are close to GOE. For large values of the interaction strength (lower panel in figure 7) a band structure develops in the energy spectrum. The ratio shows stronger fluctuations[9] and a slight drop from a more Wigner–Dyson-like value towards a more Poisson-like value.

In addition to the distributions discussed above, the Shannon entropy can give interesting information about the chaoticity of the system [22]. The Shannon entropy is defined by $S_n = (-\sum_m |c_m^n|^2 \ln |c_m^n|^2)/\ln \dim H$, where $c_n^m$ are the coefficients of the $n$th eigenstate decomposed onto the $m$th basis state of a chosen basis. The entropy measures the delocalization of a wavevector with respect to a chosen basis: with our definition, it reaches 1 for a fully delocalized state. Here we measure the entropy with respect to the symmetrized real-space basis of exact diagonalization. In figure 8 the behavior of the entropy is shown for different interaction strengths. A clear evolution from a smooth to a sharp distribution around high values at small interaction strength towards a strongly fluctuating distribution at low values is evident. This shows that, for small interaction strength, almost all eigenvectors are delocalized as expected in the non-interacting regime where the Hamiltonian is diagonal in the momentum space. At

[9] The ratio and its fluctuations also depend more strongly on the energy interval used. However, we checked that the main trend remains for typical energy ranges taken.

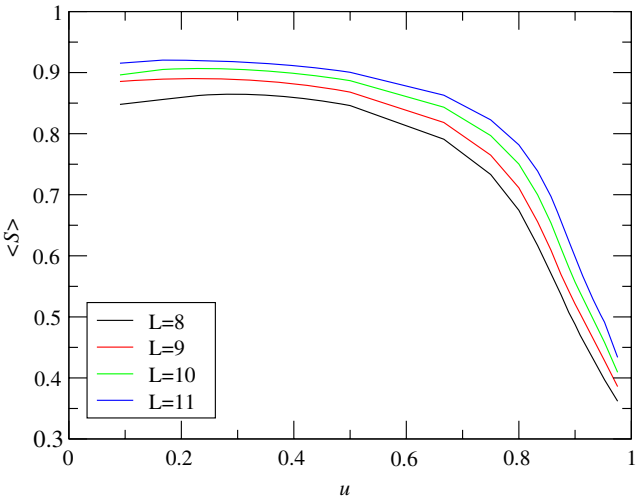


**Figure 9.** The finite system dependence of the average value of the Shannon entropy is shown. A clear trend towards larger values is found.

intermediate interaction strength, the edges display less delocalized features than in the bulk. The most interesting behavior is exhibited at large interaction strength where the degree of localization fluctuates strongly between different eigenvectors within a Mott lobe. Let us point out that this finding is similar to the behavior of some observables and weights calculated in these eigenstates and that was identified to be the reason of non-thermalization after a quench on such finite size systems [18]–[20]. Finally, let us comment on the evolution of the above results on increasing the system size. We find that, even though figure 9 displays a trend towards delocalization, the behavior in the thermodynamic limit is particularly hard to access close to the infinite-$U$ integrable point.

## 3. Perturbing the Bose–Hubbard model

We now turn to the effect of the $J_2$ and $V$ perturbations (separately) that are expected to help in breaking integrability at the $J = 0$ and $U = 0$ integrable points, respectively. As there are three parameters ranging from zero to infinity, we will fold the parameter space using two representations (see figure 10 for an example). The first one is to introduce the function $f(x, y) = x/(x + y)$ and to use the following definition: $u = f(U, J)$ and $j_2 = f(J_2, J)$, when $J \neq 0$; $u = f(U, J_2)$ and $j_2 = f(J_2, U)$ if $J = 0$, with the additional point $u = j_2 = 1$ when $U = J_2$. Such a folding is useful to restrict the considered parameters onto a finite interval, and enables one to easily deduce the parameters for a given point. One disadvantage of this folding is discontinuities arising from the infinities on the $j_2 = 1$ and $u = 1$ lines. A continuous way to draw the data is to use a ternary plot[10]. However, it is more difficult to find in such a plot the original parameters. Therefore, we use both ways to present our results.

[10] Formally speaking, a point of the diagram corresponds to a percentage of each parameter, i.e. a triplet $(\%J, \%J_2, \%U)$. In Cartesian coordinates with the triplet (100,0,0) at the origin, one has $x = (U + J_2/2)/\mathcal{N}$ and $y = \sqrt{3}J_2/2\mathcal{N}$ with $\mathcal{N} = J + J_2 + U$.



J. Stat. Mech. (2010) P08011

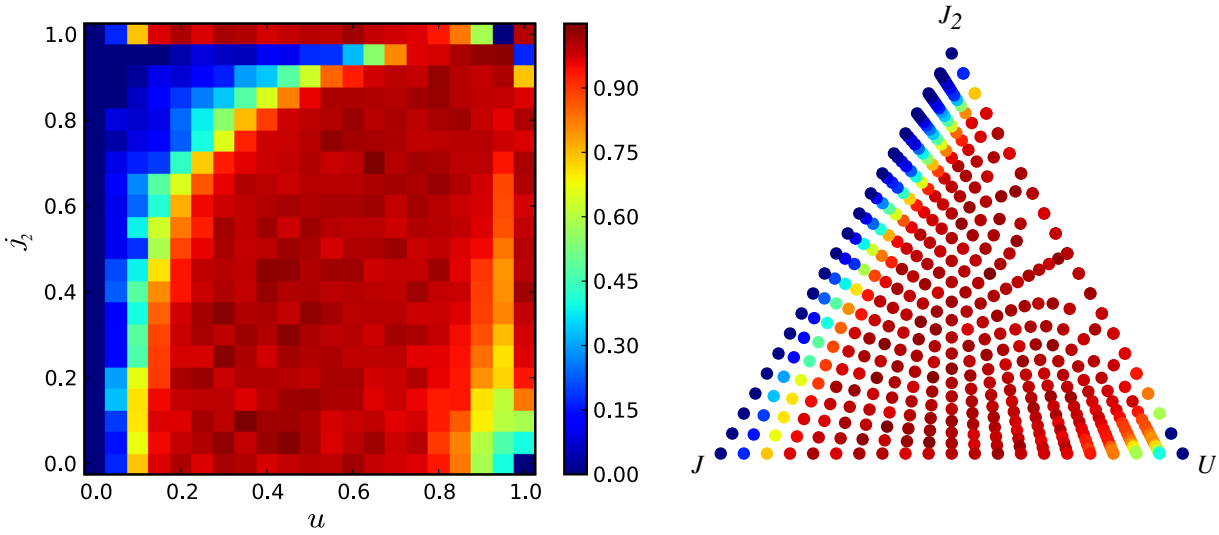


**Figure 10.** Density plots of the evolution with the parameters $j_2$ and $u$ (see text) of the averaged ratio of consecutive level spacings $\langle r\rangle$ ($L = 11$). We plot $(\langle r\rangle - \langle r\rangle_{\mathrm{P}})/(\langle r\rangle_{\mathrm{P}} - \langle r\rangle_{\mathrm{GOE}})$, so that blue (resp. red) corresponds to Poissonian (GOE) distribution. Right panel: ternary plot of the same data showing the integrable lines $J - J_2$ and the isolated integrable point ($U$ corner).

### 3.1. Influence of a next-nearest-neighbor hopping

If the next-nearest-neighbor hopping $J_2$ is switched on, the behavior of the spectrum changes. A summary of the effect of $J_2$ for $L = 11$ is presented in figure 10. For small and intermediate interaction strength, the additional finite value of $J_2$ drives the small systems closer to the Poisson behavior. For large interaction strength, $J_2$ helps to drive the system away from the integrable point $J = 0$, before at very large $j_2$ it again turns Poisson-like due to the attraction of the $U = J = 0$ integrable point. The values of $J_2$ can thereby be much smaller than the actual interaction strength and still have a considerable influence. In the ternary diagram the almost symmetric behavior of the system with respect to the diagonal $J = J_2$ is nicely visible. This means that the next-nearest-neighbor hopping $J_2$ has a similar effect as the nearest-neighbor hopping $J$. In order to discuss the influence of longer system sizes, we show in figure 11 the dependence of the average ratio $\langle r\rangle$ on $j_2$ for different system sizes at chosen values of the interaction strength. If the behavior is already close to the GOE one, finite size effects are typically very small (figure 11, central panel). In contrast, if the system is not in the GOE regime, the finite size effects become more pronounced. However, the larger system sizes show a clear tendency towards the GOE behavior. Lastly, we have checked that the same qualitative features are displayed in the Shannon entropy when $J_2$ is taken into account. For instance, figure 12 shows that starting from a large $U/J$ and increasing $J_2$ tends to make the wavefunctions delocalize in the symmetrized real-space basis of exact diagonalization. In particular, for the point with $J = J_2$, the perturbation clearly favors delocalization. When $J_2/U$ increases, the delocalization with respect to the real-space basis becomes more and more pronounced due to the dominating kinetic term. As for the case of the pure Bose–Hubbard model, a strong dependence on the energy is observed. A maximum in the Shannon entropy is

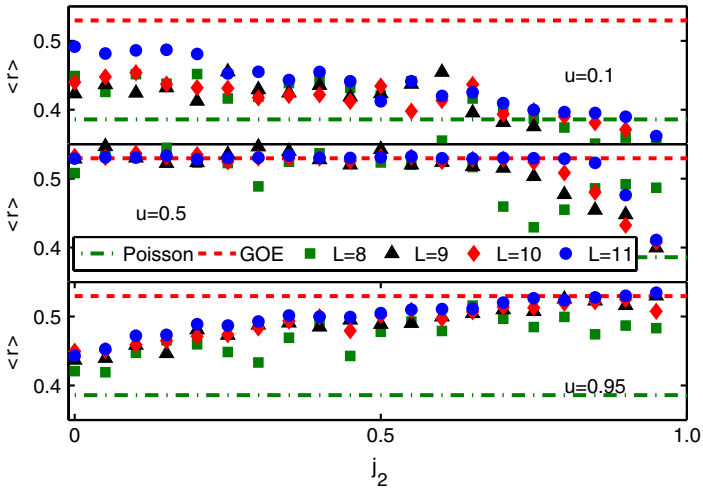


**Figure 11.** Evolution of the ratio of consecutive level spacings $\langle r \rangle$ with nn hopping $j_2$ for different interaction strengths. For the Poisson distribution the average value of $\langle r \rangle_{\mathrm{P}} = 0.386$ and for the GOE ensemble $\langle r \rangle_{\mathrm{GOE}} = 0.53$ are displayed. The average is taken for the full spectrum, without cutting the low and the high energy part (circles).

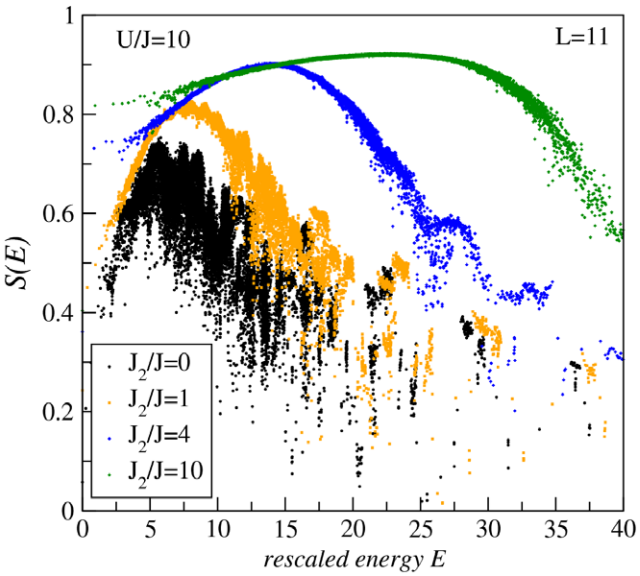


**Figure 12.** Effect of the $J_2$ perturbation on the Shannon entropy in the symmetrized real-space basis.

found for intermediate energies, whereas for low and in particular high energy the Shannon entropy drops quickly and exhibits typically more fluctuations.

### 3.2. Influence of the nearest-neighbor interaction

In the following paragraph we discuss the influence of nearest-neighbor interactions which is summarized in figure 13. The same representations of the parameters space are taken,

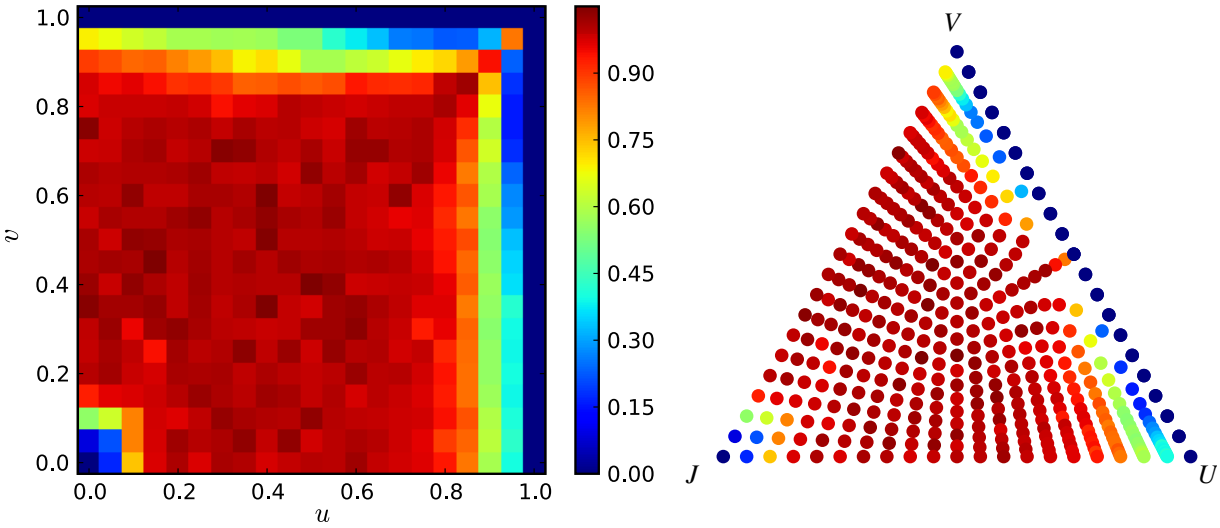


**Figure 13.** Same as figure 10 changing $J_2$ with nearest-neighbor interaction $V$.

replacing $J_2$ with $V$ and $j_2$ with $v$. The behavior is qualitatively very different from the $J_2$ perturbation: the integrable line in the ternary plot is now the $U - V$ line. In both representations, the data are nearly symmetrical with respect to the diagonal $U = V$. Thus, the two interacting terms act in a similar way in terms of level statistics. For small onsite interaction strength $U$, a finite nearest-neighbor interaction $V$ enhances the trend of the ratio towards its GOE value. However—surprisingly at first sight—at large onsite interaction strength $U$, a small finite value of $V$ induces a trend towards the GOE-like behavior and only if $V$ is larger than the onsite interaction $U$ the value of the ratio drops drastically to the Poisson value. In particular, for interactions of the same order of magnitude $U \sim V$, $J$ rapidly drives the system towards GOE. This effect can be made plausible in a simplified picture considering the eigenstates of the Hamiltonian at $J = 0$, which are Fock states. However, their order with respect to the energies is very different for both interactions. To make this more explicit consider the state with one particle per site $|1\rangle = |1, 1, \ldots, 1\rangle$ and the state with two particles every second site $|2\rangle = |2, 0, 2, 0, \ldots, 2, 0\rangle$. For a strong onsite interaction the state $|1\rangle$ is very low in energy whereas the state $|2\rangle$ lies in the upper part of the spectrum. In contrast, for a strong nn-interaction state $|2\rangle$ lies in the lower part of the spectrum whereas state $|1\rangle$ lies in the upper part. If both interactions are of the same order of magnitude both states lie very close in energy such that the small hopping has a large effect on the states. These two energy states are examples of the behavior of many of the energy states which become almost degenerate in the limit of equal onsite and nn-interaction strength. Therefore, the effect of the hopping as a perturbation is expected to be more effective when $U \sim V$ and should help make the level statistics GOE-like.

In figure 14, finite size effects are considered. As for the other cases discussed the finite size effects are very small if the value of the ratio is already close to GOE. For the remaining values, we typically see a trend of the ratio for larger system sizes towards GOE.

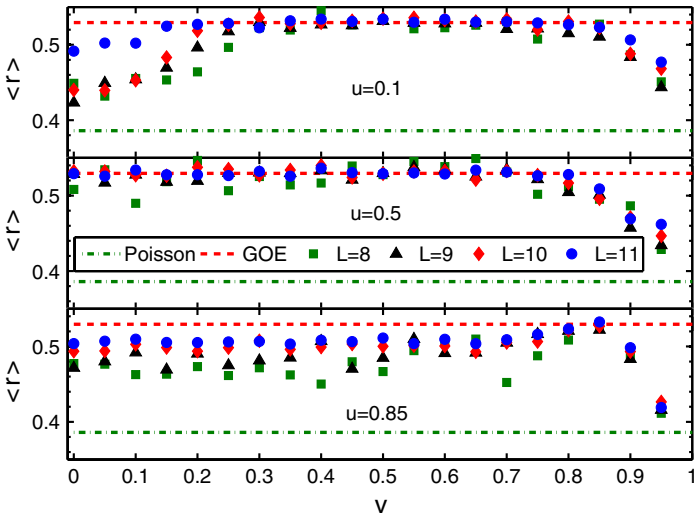


**Figure 14.** Same as figure 11 changing $J_2$ with nearest-neighbor interaction $V$.

### 3.3. Occupation cutoff dependence

In figure 15, we show the effect of introducing a cutoff in the number of bosons $M$ on each site. For large values of the interaction strength the use of a cutoff $M > 4$ does not seem to change the spectral properties much, both at unit and half-fillings. A smaller cutoff strongly affects the ratio, pushing it close to the GOE prediction. This is due to the suppression of the remaining particle fluctuations mixing the true eigenstates which are no longer represented. For intermediate interaction where the ratio is close to the GOE value, the effect of the cutoff on the mean ratio is relatively small. In contrast for small interaction strength the influence of the cutoff is very pronounced. Here the introduction of a small cutoff does drive the system away from integrability. Even for $U = 0$, using $M < N$ makes the level statistics close to GOE. This effect can be understood by recalling the properties of the eigenstates in the limit of weak interaction. These are the momentum eigenstates which comprise strong particle fluctuations. If one introduces a cutoff for the number of bosons per site these states cannot be represented anymore and start to mix. In other words: the local constraint is equivalent to using a projector on the kinetic part which correlates the bosons or, equivalently, acts as a complicated effective interaction that turns out to display a GOE behavior. A qualitatively similar effect is found in the comparison between the 1D $t$–$J$ and Hubbard model. The Hubbard model is integrable while the $t$–$J$ model, which is related to the Hubbard model by Gutzwiller's projection, is generically not [12].

In addition, we can discuss earlier results in the literature addressing the question of the integrability of the 1D Bose–Hubbard model and the effect of multi-occupancies. Seminal studies by Choy and Haldane [28, 29] seemed to argue that Bethe-ansatz equations yield solutions of Bose–Hubbard-like models but the analysis turned out to be invalid [30, 31]. The authors emphasized that $M > 3$ was required to give rise to non-integrability. Later, Krauth [32] used the Bethe-ansatz wavefunction as a variational approach for the ground state properties. He found that, for $U/J \lesssim 2$, the comparison with

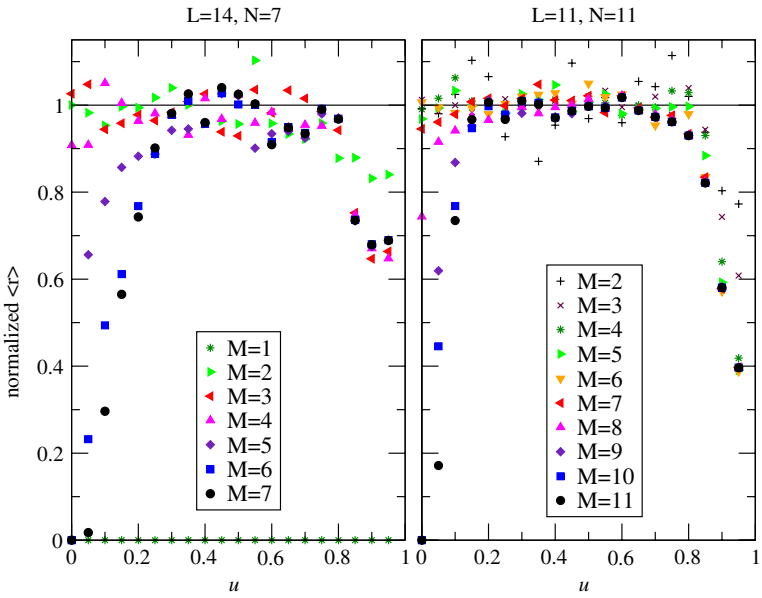


**Figure 15.** Evolution of $(\langle r\rangle - \langle r\rangle_{\mathrm{P}})/(\langle r\rangle_{\mathrm{P}} - \langle r\rangle_{\mathrm{GOE}})$ with the maximum number of onsite bosons $M$. The average is taken for the full spectrum, without cutting the low and the high energy parts (circles). Left panel: incommensurate density where hard-core bosons correspond to $M = 1$. Right panel: the same at a commensurate density $N = L$.

unbiased quantum Monte Carlo results was indeed very good. This finding supported the fact that the integrable nature of the free boson gas was preserved up to interactions close to the transition point to the Mott insulating phase at least for ground state properties. The results of the present study, in which we found by considering the entire spectrum that the chaotic properties emerge much below $U/J \simeq 2$ ($u \simeq 0.66$), stress the difference between the low energy part of the spectrum and high energy regions: the ground state and first excitations might have integrable-like behavior (if the density of quasi-particles is small, they may interact less) while one cannot consider a high energy excitation as simply being made of a superposition of elementary excitations [11] (a picture which survives high in energy in the Bethe ansatz and in free-particle systems).

## 4. Conclusion

To conclude, we presented a study of the characteristic properties of the spectra of the extended Bose–Hubbard model. In an intermediate regime of the interaction strength the system is in the GOE regime. In contrast, for very weak and strong interaction strength the analysis suggests an approach toward GOE when increasing system sizes. In most parameter regimes this trend towards the GOE was most pronounced in the central region of the spectrum. An additional next-neighbor hopping amplitude $J_2$ changes the properties of the energy levels in these small systems. It acts similar to the hopping amplitude $J$. For weak interaction, $J_2$ drives the system closer to the Poisson-like behavior, whereas for large interaction strength it reinforces the GOE-like behavior. An additional



J. Stat. Mech. (2010) P08011

nearest-neighbor interaction $V$ has a similar effect on the statistical properties of the spectrum as the onsite interaction even though the corresponding eigenstates are very differently distributed in energy. Close to the point where the interaction $U$ and $V$ become of similar strength even a very small value of $J$ is enough to induce a GOE-like statistics. Finally we discussed the influence of the introduction of a cutoff for the number of bosons per site usually used to render the system numerically tractable. Here we see that the cutoff can change the statistics of the spectrum from Poisson-like to GOE-like, in particular at small interaction strength.

We see that for all the different regimes considered the changes with increasing system size can be divided into two main classes. If the properties of the system are already GOE-like, increasing the system size only induces small changes. In contrast, if the value of the ratio of consecutive level spacings lies in between the Poisson and the GOE value, indicating a mixed statistics, finite size effect are considerable. In this regime larger system sizes typically drive the system towards the GOE value indicating a GOE-like behavior in the thermodynamic limit. However, larger sizes would be needed to obtain a conclusive result on the question of whether there is always a large enough system size to reach a GOE behavior for all parameters except the ones corresponding to the integrable points (or lines) or if a threshold for the perturbation from the integrable point exists to reach it.

## Acknowledgments

We would like to thank B Altshuler, N Andrei and A Millis for fruitful discussions. This work was partly supported by the 'Triangle de la Physique', DARPA-OLE, and the ANR ('FAMOUS').

## References

[1] Haake F, 2000 *Quantum Signatures of Chaos* (Berlin: Springer)
[2] Peres A, 1984 *Phys. Rev.* A **30** 1610
[3] Peres A, 1984 *Phys. Rev.* A **30** 504
[4] Kota V K B, 2001 *Phys. Rep.* **347** 223
[5] Bloch I, Dalibard J and Zwerger W, 2008 *Rev. Mod. Phys.* **80** 885
[6] Kinoshita T, Wenger T and Weiss D S, 2006 *Nature* **440** 900
[7] Brody T A, Flores J, French J B, Mello P A, Pandey A and Wong S S M, 1981 *Rev. Mod. Phys.* **53** 385
[8] Bohigas O and Giannoni M, 1986 *Quantum Chaos and Satistical Nuclear Physics* (*Lecture Notes in Physics* vol 263) (Berlin: Springer)
[9] Mehta M L, 1991 *Random Matrices* 2nd edn (New York: Academic)
[10] Guhr T, Mueller-Groeling A and Weidenmueller H A, 1998 *Phys. Rep.* **299** 189
[11] Montambaux G, Poilblanc D, Bellissard J and Sire C, 1993 *Phys. Rev. Lett.* **70** 497
[12] Poilblanc D, Ziman T, Bellissard J, Mila F and Montambaux G, 1993 *Europhys. Lett.* **22** 537
[13] Sutherland B, 2004 *Beautiful Models* (Singapore: World Scientific)
[14] Hsu T C and Anglès d'Auriac J C, 1993 *Phys. Rev.* B **47** 14291
[15] Prosen T, 1999 *Phys. Rev.* E **60** 3949
[16] Kollath C, Läuchli A M and Altman E, 2007 *Phys. Rev. Lett.* **98** 180601
[17] Läuchli A M and Kollath C, 2008 *J. Stat. Mech.* P05018
[18] Roux G, 2009 *Phys. Rev.* A **79** 021608
[19] Roux G, 2010 *Phys. Rev.* A **81** 053604
[20] Biroli G, Kollath C and Läuchli A, 2009 arXiv:0907.3731
[21] Jaksch D, Bruder C, Cirac J I, Gardiner C W and Zoller P, 1998 *Phys. Rev. Lett.* **81** 3108
[22] Kolovsky A R and Buchleitner A, 2004 *Europhys. Lett.* **68** 632
[23] Bodyfelt J D, Hiller M and Kottos T, 2007 *Europhys. Lett.* **78** 50003
[24] Hiller M, Kottos T and Geisel T, 2009 *Phys. Rev.* A **79** 023621



J. Stat. Mech. (2010) P08011

[25] Santos L F and Rigol M, 2010 *Phys. Rev.* E **81** 036206
[26] Oganesyan V and Huse D A, 2007 *Phys. Rev.* B **75** 155111
[27] Cassidy A C, Mason D, Dunjko V and Olshanii M, 2009 *Phys. Rev. Lett.* **102** 025302
[28] Choy T C, 1980 *Phys. Lett.* A **80** 49
[29] Haldane F D M, 1980 *Phys. Lett.* A **80** 281
[30] Haldane F D M, 1981 *Phys. Lett.* A **81** 575
[31] Choy T C and Haldane F D M, 1982 *Phys. Lett.* A **90** 83
[32] Krauth W, 1991 *Phys. Rev.* B **44** 9772

J. Stat. Mech. (2010) P08011